

PARAMETRIC ANALYSIS OF CFRP STRIPS INTERNALLY CONFINED RC COLUMNS

Nur Hajarul Falahi Abdul Halim^{a*}, Sophia C. Alih^b,
Mohammadreza Vafaei^b

^aFaculty of Built Environment & Surveying, Universiti Teknologi
Malaysia, 81310 UTM Johor Bahru, Malaysia

^bFaculty of Civil Engineering, Universiti Teknologi Malaysia,
81310 UTM Johor Bahru, Malaysia

Article history

Received

14 August 2023

Received in revised form

2 November 2023

Accepted

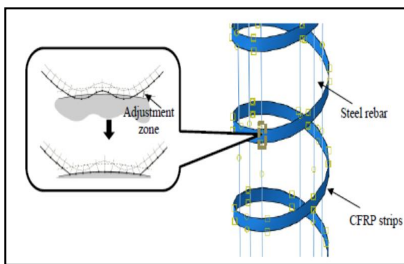
5 November 2024

Published Online

20 August 2024

*Corresponding author
nurhajarulalahi.ah@utm.my

Graphical abstract



Abstract

Fiber-reinforced polymer (FRP) sheets has been widely used as external confinement for retrofitting and strengthening structural elements as they increase axial, shear, and bending capacity. Despite many advantages, FRPs suffer from some drawbacks such as have weak durability against thermal and harsh environment. Thus, the use of FRP strips as internal confinement was proposed so that the concrete cover can protect the FRP strips. In this study, a three-dimensional (3D) nonlinear finite element (FE) model is developed using ABAQUS software to study the cyclic behavior of carbon fiber-reinforced polymer (CFRP) strips internally confined reinforced concrete (RC) columns. A validated model was used to conduct the parametric study to investigate the effect of FE model under different intensities of axial load (i.e. 70kN, 100kN, 200kN, 300kN, and 400kN) and distances between the CFRP spirals (100mm, 150mm, 200mm, and 250mm). Results indicate that an increase in the axial force has significantly increased the stress on the surface of concrete and can lead to the rupture of CFRP strips in the column. Meanwhile, increasing the distance between CFRP strips has increased the stress at the plastic hinge area and experienced buckling of longitudinal reinforcements at 250 mm of CFRP strips.

Keywords: CFRP, quasi-static cyclic load, finite element modelling

Abstrak

Lapisan polimer bertetulang gentian (FRP) telah digunakan secara meluas sebagai kurungan luar untuk pengubahsuaian dan mengukuhkan elemen struktur kerana ia meningkatkan beban paksi, ricih dan lenturan. Walaupun terdapat banyak kelebihan, FRP mengalami beberapa kelemahan seperti mempunyai ketahanan yang lemah terhadap terma dan persekitaran yang keras. Oleh itu, penggunaan jalur FRP sebagai kurungan dalaman dicadangkan supaya lapisan luar konkrit dapat melindungi jalur FRP. Dalam kajian ini, model tiga dimensi (3D) unsur terhingga tak linear dibangunkan menggunakan perisian ABAQUS untuk mengkaji kelakuan kitaran tiang konkrit bertetulang (RC) secara dalaman terkurung oleh jalur polimer bertetulang gentian karbon (CFRP). Kerja pengesahan model dilakukan sebelum menjalankan kajian parametrik selanjutnya untuk menyiasat kesan model FE di bawah keamatan beban paksi yang berbeza (iaitu 70kN, 100kN, 200kN, 300kN dan 400kN) dan jarak antara lingkaran CFRP (100mm, 200mm, 100mm, dan 250mm). Keputusan menunjukkan bahawa peningkatan dalam daya paksi telah meningkatkan tegasan pada permukaan konkrit dengan ketara dan boleh menyebabkan pecahnya jalur CFRP dalam lajur. Sementara itu, meningkatkan jarak antara jalur CFRP telah meningkatkan tegasan pada kawasan engsel plastik dan mengalami lengkakan tetulang membujur pada 250 mm jalur CFRP.

Kata kunci: CFRP, beban kitaran kuasi-statik, pemodelan unsur terhingga

© 2024 Penerbit UTM Press. All rights reserved

1.0 INTRODUCTION

Fibre reinforced polymer (FRP) sheets have been widely used for retrofitting and strengthening reinforced concrete (RC) structures. Their high strength-to-weight ratio, high durability to harsh environment, lightweight and ease of installation make them good options to engineers and contractors as compared to the conventional method which uses RC jacketing. FRP sheets have been successfully used to enhance the flexural and shear strength of concrete structures [1], [2]. Besides, FRPs have increased the seismic performance for the ultimate load, ductility and energy dissipation capacity of concrete members [3], [4]. For instance, Shin *et al.* [5] retrofitted RC columns with hybrid FRP (HFRP) sheets by using carbon and glass fibre and tested under cyclic loading. The study reported that wrapping HFRP sheets enhanced the cracking and ultimate load of columns. In addition, wrapped columns with two plies of HFRP enhanced at least 2.1 times deformation capacity as compared to unwrapped columns. Zhang *et al.* [6] employed FRP sheets as external confinement for rectangular concrete columns. The study showed that rectangular columns with aspect ratio from 1.0 to 2.0 had excellent seismic response and ductility. Moreover, it concluded that the increase in FRP thickness could enhance the peak lateral load of columns.

In addition, FRP sheets have been successfully employed for repairing corroded reinforced structures. For instance, Zhou *et al.* [7] retrofitted corroded steel reinforcement in RC columns by using polyethylene terephthalate (PET) FRP with large rupture strain (LRS). The study reported that LRS-FRP significantly improved the ductility and energy dissipation capacity of corroded RC columns. Li *et al.* [8] employed LRS-FRP for repairing corroded RC columns and addressed that the external confinement could effectively enhance the performance of corroded columns. However, the compressive strength and ductility of repaired RC columns were significantly affected by the existence of corrosion, which weakened the rebar sections and further damaged the confined concrete. In addition to this issue, despite the high strength and flexibility of FRP sheets, a literature review showed that the elevated temperature and harsh environment could significantly decrease the tensile strength of FRPs and lead to debonding of the fibres [9], [10]. Therefore, many efforts were made to address the debonding of FRP, for example, by applying surface treatment method, such as by using the groove anchorage method [11], [12].

Despite many efforts that were made to improve the bond between the FRP and concrete joints, it was shown that to maintain quality of bond surface for the entire structure was challenging. This outcome is mainly because improving the quality of the bonding surface is expensive, time-consuming and requires excellent workmanship [9], [10], [13]. Therefore, one way to reduce the adverse effects of high temperatures and harsh environments on FRPs and its

bond strength is to use FRPs for internal confinement. In this way, the concrete cover can protect FRP from high temperatures and harsh environments. Motivated by this idea, this present study investigated experimentally the cyclic behaviour of FRPs as internal reinforcements in RC columns [14]. Comparisons were made between the response of the reference columns, which were confined with steel spirals. The results indicated RC columns that transversely reinforced with CFRP strips had a larger ultimate load, displacement ductility ratio and effective yield strength as compared to the reference columns. Besides, CFRP strips reduced the number of cracks on the concrete surface when compared with the reference columns. The length of cracks in CFRP confined columns were also relatively shorter.

Finite element modelling (FEM) can excellently demonstrate the micromechanical characteristic of composite material. Due to time constraints in conducting the experimental work, this study presented a comprehensive numerical analysis by developing a finite element model of RC columns internally confined by FRP strips. The aim of this study is to investigate the effect of different axial load intensities (70 kN, 100 kN, 200 kN, 300 kN and 400 kN) and different distances between the FRP strips (100 mm, 150 mm, 200 mm and 250 mm).

2.0 FINITE ELEMENT MODELLING

Figure 1 shows the selected research methodology for this study. Finite element analysis software ABAQUS [15] was used in this study to develop a nonlinear finite element model. ABAQUS/Standard was selected due to its ability in solving various linear and nonlinear problems for static and dynamic loads. Additionally, this software can simulate stress in the CFRP strips.

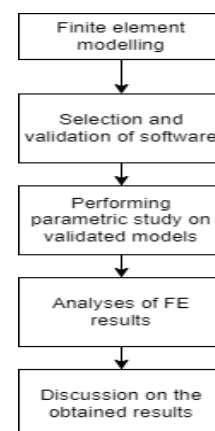


Figure 1 Selected research methodology

2.1 Material Properties

Analysis of internally confined CFRP strips in RC columns presented many challenges due to the

composite action of different components (concrete, steel, FRP). This non-linear analysis was conducted by using existing laws and mechanical properties that illustrate the actual mechanical properties and boundary condition of the laboratory tests. The properties of concrete, steel and CFRP were adopted from laboratory studies, as shown in Table 1 [14]. Concrete of 25 MPa compressive strength was used in this study together with 563 MPa and 4900 MPa tensile strength of steel and CFRP strips, respectively.

Table 1 Mechanical properties of materials

Material	Compressive strength (MPa)	Tensile strength (N/mm ²)	Modulus of elasticity (N/mm ²)	Poisson's ratio
Concrete	25	-	-	0.2
Steel	-	563	200,000	0.3
Carbon	-	4900	252,000	-

2.2 Model Geometry and Element Types

For many studies, a 2D model may provide accurate and less time-consuming results. However, in this study, a 3D solid model should be developed so that more details could be included in the models. The columns were modelled by using an eight-node 3D brick element (C3D8R) with three degrees of freedom per node to simulate the non-linear properties of concrete elements. This method was similar with what was done by Zhang *et al.* [16] and Kyaure *et al.* [17] to model RC columns with composites material. The embedded reinforcing steel was modelled by using a two-node linear 3D truss (T3D2). This option was used to specify the plastic part of material model for elastic-plastic materials, such as steel. Meanwhile, CFRP strips were modelled by using a 3D shell element, which was a four-node general-purpose shell element and was named finite membrane strains (S4R). The conventional shell elements were used to model structures in which one dimension was significantly smaller than the others. The number of CFRP ply was defined with thickness of 0.164 mm. The rotation angles of 90° were selected to define the direction of fibres along the direction of spirals.

Next was to determine the contact behaviour between elements. In ABAQUS, the embedded element technique was used to model a set of rebar-reinforced members that lied embedded in a set of 3D solid elements. Therefore, the embedded technique was used to demonstrate the contact between reinforcing steel bars and concrete elements. Meanwhile, surface-to-surface with cohesive behaviour was selected to simulate the interaction between CFRP strips and steel bars. To avoid any initial overclosures or gaps between the nodes, ABAQUS has provided some tools for adjusting slave nodes in a contact pair so that they precisely contact the master surface, as shown in Figure 2.

Slave nodes that are over closed in the initial configuration may cause convergence problems.

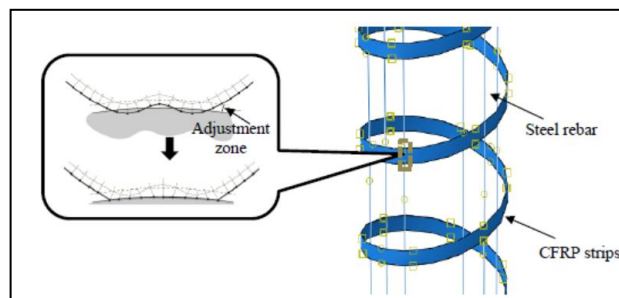


Figure 2 Contact surface between CFRP strips and steel bars

2.3 Boundary Conditions and Mesh Configuration

In this study, the boundary conditions and direction of loading were employed according to literature, as illustrated in Figure 3 [14]. A rigid support condition was adopted for joints at the bottom of the simulated foundation, representing the foundation blocks of laboratory samples that were fully fixed to the ground floor. A static general step was modelled by applying a linear increasing displacement of 0.01 mm step increment. A point load was selected to simulate a constant axial load applied at the centre of the plate placed on top of the column, as shown in the figure. Meanwhile, a displacement control was applied to the direction of x-axis at the reference point that marks as lateral load, which will impose a cyclic lateral load to the FE model. The steps for cyclic loading were included in the amplitude, in which each cycle should be repeated twice with an increasing amplitude of 40% as compared to its previous cycle until the target displacement was reached.

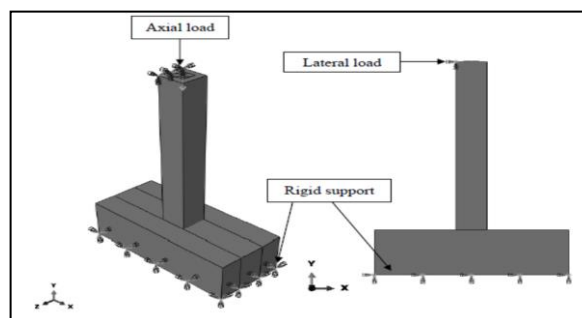


Figure 3 Boundary conditions adopted from [17]

Mesh sensitivity analysis was conducted by using different mesh sizes, ranging between 10 mm and 40 mm. The selection of mesh size is important to reduce the potential of convergence issues during analysis. The analysis revealed that finer mesh sizes (10 mm and 15 mm) were suitable for smaller configuration of materials, while coarse mesh sizes (20 mm – 40 mm) were compatible for larger elements. Figure 4 shows

the FE model of concrete and reinforcements with meshing. Course meshes of up to 40 mm were used for concrete sections and reinforcements steel bars, while for CFRP strips a fine mesh of up to 15 mm was used.

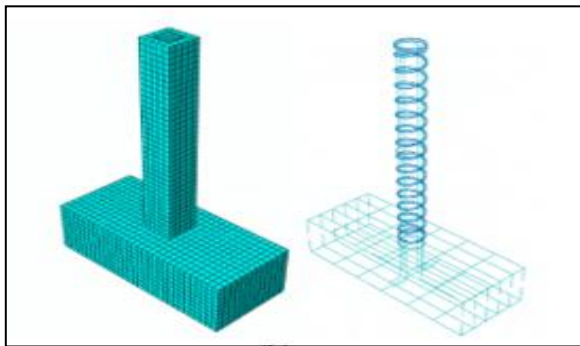


Figure 4 Meshing for concrete and reinforcements

3.0 MODEL VALIDATION

Before conducting the parametric study, a numerical analysis was conducted and compared with the results obtained from the experimental works to verify the FE model. Validation of the established FE model was achieved by comparing force-displacement relations and failure mode of the columns.

Figure 5 presents the comparison of force-displacement curves between the FE model and experimental test. The configurations of FRP strips, size and dimension of columns and loading protocol of the FE model were similar with the experimental test from literature [14]. Results showed that the initial stiffness obtained from FE model was 1.38 kN/mm, which was 10% smaller than the results of experimental test (1.53 kN/mm). Besides, the FE model showed an ultimate load and displacement of 31.1 kN and 94.2 mm, respectively. This means a 7% difference in ultimate load capacity and 3% difference in the displacement of FE model and experiment.

Figure 6 displays the concentration of stress along the height of columns and compares them with the results of FE model. Red colour represents higher stress values on the concrete surface. As can be seen from the figures, the FE model could capture similar stress concentration as shown in the test results.

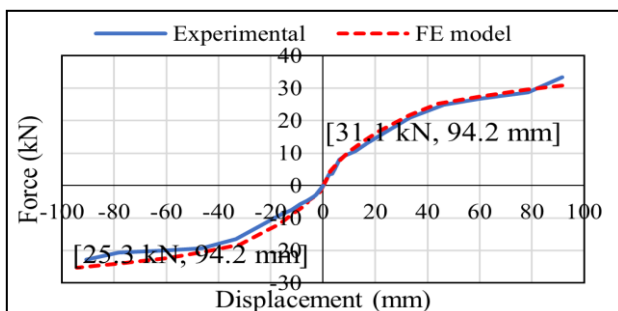


Figure 5 Comparison between force-displacement relationship of FE model and experimental test

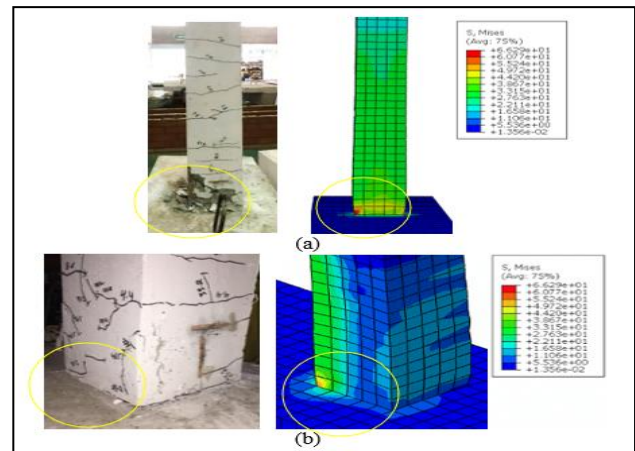


Figure 6 Comparison of stress distribution between FE model vs experimental (a) left side of column and (b) bottom of column

Table 2 shows a summary of the obtained results for the initial stiffness, ultimate lateral load and its corresponding displacement. As can be seen, the FE model had precisely estimated the ultimate lateral load and their corresponding displacement. The initial stiffness of columns was overestimated by the FE model with a maximum difference of 10%. This could be due to the employed mesh size as it had been reported by other researchers [18]. In addition, the support condition in the FE models was assumed to be fixed. However, in the laboratory tests the supports were not completely fixed. The ultimate of test specimens and their corresponding displacements were also estimated by the FE models with error of less than 10%. Moreover, the stress distributions on the concrete surface correlated well with those observed from the experiment. Therefore, the FE models could be used for further analysis.

Table 2 Comparison between initial stiffness, ultimate lateral load, and its corresponding displacement

	FE model	Experimental
Initial stiffness (kN/mm)	1.38	1.53
Ultimate load capacity (kN)	31.1	33.4
Ultimate displacement (mm)	94.2	91.6

4.0 PARAMETRIC STUDY

The main aim of this section was to study the effect of higher intensities of axial load and difference in distance between CFRP strips on the cyclic behaviour of columns internally confined by CFRP strips. It should be mentioned that this parametric study was simulated by using the same dimension and configurations of column and arrangements of reinforcements steel and FRP spirals, as shown in Figure 7. The same loading protocol of lateral load

was also employed as per the experimental study. However, for the first purpose, the FE model was subjected to 100 kN, 200 kN, 300 kN and 400 kN together with the cyclic lateral load used in the experimental study. It should be mentioned that the axial load was considered based on the axial load ratio (0.75 ~ 2.00).

For columns confined with carbon steel, the larger distance between the stirrups could result in a significant decrease in strength and ductility due to buckling of longitudinal bars and shear failure [19]. Furthermore, seismic codes like Eurocode 8 have limited the distance between stirrups as one of main parameters for seismic design of RC columns. Therefore, by using a constant axial load and cyclic lateral loading, the second purpose was to investigate its effect on the cyclic response of column by increasing the distance between stirrups to 200 mm and 250 mm.

5.0 RESULTS AND DISCUSSION

5.1 Effect of Different Intensities of Axial Load

Figure 7 shows stress distributions on the concrete surface, steel bars and CFRP strips of the FE model at an axial load of 400 kN. Stress values were taken at the central area near the bottom of the column. Stress distributions on the surface of the column were shown at a 5% drift ratio.

From the results, stress values on the concrete surface of columns increased as intensity of the axial load was increased. Moreover, by increasing the intensity of axial force, the area on the concrete surface with large stress expanded along the height of columns. As compared to the column with axial force of 70 kN, the maximum stress on the concrete surface of columns with the axial force of 100 kN, 200 kN, 300 kN and 400 kN, was 13%, 21%, 26% and 33% larger, respectively. It should be mentioned that all columns had passed the compressive strength of concrete (25 MPa). The high stress zones were mostly concentrated at the bottom to the mid-height region. This result was similar to the findings of a previous experimental study on FRP spirally confined concrete columns [20]. The columns failed due to the rupture of FRP and led to a larger region of failed concrete in the column.

At 5% drift in all columns, some of the longitudinal bars have passed the yield strength of the steel bars (563 MPa). However, no buckling occurred in the longitudinal bars, except for columns with axial force of 400 kN. The longitudinal bars buckled at almost 6% drift ratio. It can also be seen that the stress distribution in the longitudinal bars was not similar and some of the longitudinal bars had not reach the yield strength. In columns with 300 kN and 400 kN axial force, the stress distribution in the CFRP spirals showed that some CFRP strips had passed the tensile strength. This finding indicated that the higher intensities of axial load had affected the failure mode of the columns.

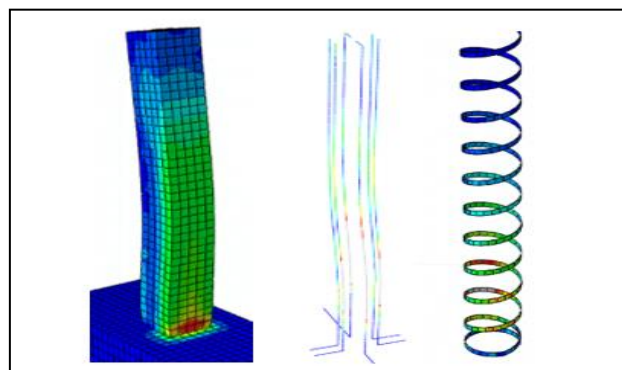


Figure 7 Stress distributions in the column at an axial load of 400 kN

Table 3 summarises the comparison of effective yield strength and ductility ratio of the FE model with different intensities of axial load. As it can be seen, the effective yield strength slightly decreased when the axial load was increased. Compared with the axial load of 70 kN, at axial loads of 100 kN, 200 kN, 300 kN and 400 kN, the effective yield strength was decreased by 0.4%, 1%, 2% and 5%, respectively. Meanwhile, the ductility ratio of columns with axial loads of 100 kN, 200 kN, 300 kN and 400 kN were 16%, 25%, 26% and 29%, smaller than that of the column with 70 kN axial force.

Table 3 Comparison of effective yield strength and ductility ratio of FE model with different intensities of axial load

Axial force (kN)	Ductility ratio	Displacement (mm)		Strength (kN)	
		Δu	Δy	F_u	F_y
70	2.31	94.20	40.80	31.11	27.50
100	1.93	90.28	46.66	31.09	27.39
200	1.74	89.11	51.11	30.94	27.16
300	1.70	66.33	38.95	29.91	26.88
400	1.65	60.74	36.84	29.66	26.22

5.2 Effect of Different Distances between CFRP Strips

Figure 8 shows the stress distributions on concrete surface, steel bars and CFRP strips of the FE model for a 250 mm distance between spirals. The stress values were taken at the centre area near the bottom of column. It is noteworthy that all columns had passed their yield stress at the 5% drift ratio.

From the results, all columns had passed the compressive strength of concrete (25 MPa). The stress distributions were increased along the height of columns as distance between the CFRP spirals was increased. High stress zones were concentrated at the bottom of the column near the foundation.

The stress intensity in the longitudinal bars was increased when the distance between spirals was increased. However, no buckling of longitudinal reinforcements was observed, except for columns with the distance of 250 mm between spirals. This

finding indicated that the provided confinement by CFRP spirals was superior even if distance between the spirals was increased up to 250 mm.

The tensile stress in the strips of columns with spirals distances of 100 mm, 150 mm and 200 mm did not reach the tensile strength of CFRP, except for 250 mm. This was similar to Djenad *et al.* [21], whereby the GFRP spirals showed the least confinement when the spacing was increased to 300 mm and 400 mm. Since FRP had brittle failure characteristic, some CFRP strips in the column with spirals distance of 250 mm had passed the maximum tensile strength of CFRP at the 5% drift ratio. This result indicated the rupture of FRP strips and led to a concrete crushing failure due to loss of confinement Zeng *et al.* [22], [23].

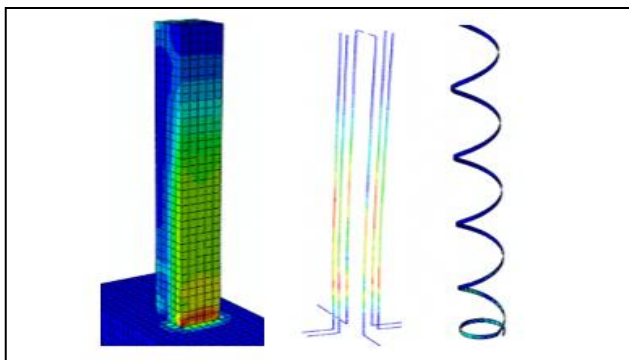


Figure 8 Stress distributions in the column at 250 mm distance between spirals

Table 4 compares the effective yield strengths and ductility ratio of columns with different distances between spirals. No significant change was observed in the effective yield strength of columns until the distance between spirals was increased to 200 mm and 250 mm. As compared to 100 mm, at spiral distance of 150 mm, 200 mm and 250 mm, the effective yield strength was decreased approximately by 7%, 23% and 35%, respectively. As compared to the 100 mm distance between spirals, for spiral distances of 150 mm, 200 mm and 250 mm, the ductility ratio was decreased by 13%, 17% and 20%. The comparison confirmed that a larger distance between the FRP spirals also affected the load capacity and ductility ratio of confined columns, as confirmed by Djenad *et al.* [21] and Daou *et al.* [24].

Table 4 Comparison of effective yield strength and ductility ratio of FE models with different distances between CFRP strips

Distance between stirrup (mm)	Ductility ratio	Displacement (mm)		Strength (kN)	
		Δu	Δy	F_u	F_y
100	2.31	94.20	40.80	31.11	27.50
150	2.02	90.26	44.79	27.12	25.62
200	1.91	92.84	48.73	22.05	21.13
250	1.84	92.78	50.54	18.86	17.89

6.0 CONCLUSION

Finite element models simulating the cyclic behaviour of CFRP spirals confined RC columns were developed. RC columns were subjected to cyclic lateral load and a constant axial load. The effect of higher intensities of constant axial loads and different distances between CFRP spirals were investigated, and conclusions were drawn.

Increase in the axial force had significantly increased stress on the concrete surface of columns. As the axial load was increased, high stress zone on the concrete surface was expanded along the height of columns. However, due to the great confinement of CFRP spirals, no buckling was observed in the longitudinal bars. Results also indicated that the increase in the axial force could lead to rupture of CFRP strips in the columns. The ultimate lateral load of columns was not significantly affected when a higher axial load was applied. However, when the axial load increased, the displacement of columns showed a reduction and corresponded to the ultimate load, leading to a decrease in the ductility ratio of columns.

Increase in distance between the CFRP strips had increased the area of plastic zone in the concrete and longitudinal bars of columns. Larger distance between CFRP strips increased the stress in the CFRP strips, especially at the plastic hinge region. The reinforcing bars of columns did not experience buckling, except for spirals with the largest distance of 250 mm. Meanwhile, columns experienced a reduction in their ultimate lateral load and effective yield strength when the distance between the CFRP strips was increased. However, no significant change was observed for displacement at the ultimate load of these columns. Besides, the ductility ratio of columns was also decreased when the distance between the strips was increased.

The outcome of this study demonstrated the efficiency of using CFRP strips as the transverse reinforcement in columns. It is suggested to investigate the bond behaviour between CFRP strips and longitudinal steel bar. It is also suggested that the developed FE methodology can be used for future parametric studies of circular FRP-confined concrete columns under cyclic loading.

Acknowledgement

The authors would like to acknowledge the Universiti Teknologi Malaysia and the Ministry of Higher Education of Malaysia for supporting this study through the research grant No. 4J224, 5F365, and 16J24.

Conflicts of Interest

The author(s) declare(s) that there is no conflict of interest regarding the publication of this paper.

References

- [1] S. Shahriari and H. Naderpour. 2020. Reliability Assessment of Shear-deficient Reinforced Concrete Beams Externally Bonded by FRP Sheets having Different Configurations. *Structures*. 25: 730-742. Doi: 10.1016/j.istruc.2020.03.048.
- [2] A. S. Abdulrahman and M. R. A. Kadir. 2022. Behavior and Flexural Strength of Fire Damaged High Strength Reinforced Rectangular Concrete Beams after Strengthening with CFRP Laminates. *Ain Shams Engineering Journal*. 13(6). Doi: 10.1016/j.asej.2022.101767.
- [3] H. Wang, G. Xing, J. Zhao, and F. Wen. Seismic Behavior of RC Columns Strengthened with Near-surface-mounted Aluminum Alloy Bars and CFRP Wraps. *Eng Struct*. 268. Doi: 10.1016/j.engstruct.2022.114742.
- [4] J. Yang, S. Liang, X. Zhu, L. Dang, J. Wang, and J. Tao. 2021. Experimental Research and Finite Element Analysis on the Seismic Behavior of CFRP-strengthened Severely Seismic-damaged RC Columns. *Structures*. 34: 3968-3981. Doi: 10.1016/j.istruc.2021.10.015.
- [5] D. H. Shin and H. J. Kim. 2020. Cyclic Response of Rectangular RC Columns Retrofitted by Hybrid FRP Sheets. *Structures*. 28: 697-712. Doi: 10.1016/j.istruc.2020.09.016.
- [6] B. Zhang, Y. Gao, H. Zheng, F. Xu, Q. Zhang, and S. Wang. 2023. Seismic Behaviour and Modelling of Rectangular FRP-concrete-steel Tubular Columns under Axial Compression and Cyclic Lateral Loading. *Structures*. 48: 1505–1518. Doi: 10.1016/j.istruc.2023.01.039.
- [7] Y. Zhou et al. 2020. Seismic Performance of Large Rupture Strain FRP Retrofitted RC Columns with Corroded Steel Reinforcement. *Eng Struct*. 216. Doi: 10.1016/j.engstruct.2020.110744.
- [8] P. Li, Y. Ren, Y. Zhou, Z. Zhu, and Y. Chen. 2022. Experimental Study on the Mechanical Properties of Corroded RC Columns Repaired with Large Rupture Strain FRP. *Journal of Building Engineering*. 54. Doi: 10.1016/j.jobe.2022.104413.
- [9] J. Liu, X. Fan, and C. Shi. 2021. Effect of Bonding Layers on Dynamic Fracture Characteristics of FRP Reinforced Concrete. *Constr Build Mater*. 309. Doi: 10.1016/j.conbuildmat.2021.125136.
- [10] F. Wang, M. Li, and S. Hu. 2014. Bond Behavior of Roughing FRP Sheet Bonded to Concrete Substrate. *Constr Build Mater*. 73: 145-152. Doi: 10.1016/j.conbuildmat.2014.09.057.
- [11] E. A. Alshuqari and A. Çevik. 2022. Behavior of Bond-Slip Relationship of Lightweight and Normal Weight Geopolymer with Various FRP Sheets using End-groove Anchorage. *Constr Build Mater*. 343. Doi: 10.1016/j.conbuildmat.2022.128060.
- [12] S. Zolfaghari, D. Mostofinejad, N. Fantuzzi, R. Luciano, and F. Fabbrocino. 2023. Experimental Evaluation of FRP-Concrete Bond using Externally-bonded Reinforcement on Grooves (EBROG) Method. *Compos Struct*. 116693. Doi: 10.1016/j.compstruct.2023.116693.
- [13] C. Chen, X. Wang, L. Sui, F. Xing, X. Chen, and Y. Zhou. (2019). Influence of FRP Thickness and Confining Effect on Flexural Performance of HB-strengthened RC beams. *Compos B Eng*. 161: 55-67. Doi: 10.1016/j.compositesb.2018.10.059.
- [14] N. H. F. A. Halim, S. C. Alih, and M. Vafaei. 2021. Seismic Behavior of RC Columns Internally Confining by CFRP Strips. *Advances in Concrete Construction*. 12(3): 217-225. Doi: 10.12989/acc.2021.12.3.217.
- [15] ABAQUS. 2014. Simulia DS. Abaqus 6.14 Documentation. Providence, RI, USA.
- [16] Y. Zhang, A. Tabandeh, Y. Ma, and P. Gardoni. 2019. Seismic Performance of Precast Segmental Bridge Columns Repaired with CFRP Wraps. *Composite Structures*. 243. Doi: 10.1016/j.compstruct.2020.112218.
- [17] M. Kyaure and F. Abed. 2021. Finite Element Parametric Analysis of RC Columns Strengthened with FRCM. *Compos Struct*. 275. Doi: 10.1016/j.compstruct.2021.114498.
- [18] M. Barker. 2018. How to Get Meaningful and Correct Results from your Finite Element Model. 1-26.
- [19] J. B. Mander, J. N. Priestley M, and R. Park. 1988. Theoretical Stress-Strain Model for Confined Concrete. *Journal of Structural Engineering*. 114(8).
- [20] G. M. Chen, M. Q. Fu, J. J. Zhang, G. Lin, J. P. Chen, and T. Jiang. 2023. FRP Spiral Strip-confined Concrete Columns: Stress-strain Behavior and Size Effect. *Structures*. 57. Doi: 10.1016/j.istruc.2023.105223.
- [21] S. Djenad, S. Ait Taleb, and A. Si Salem. 2023. Finite Element Modeling of Partially-confined Concrete and RC Columns with Embedded Hexagonal-FRP Strips under Axial and Horizontal Loading. *Structures*. 54: 369-385. Doi: 10.1016/j.istruc.2023.05.065.
- [22] J. Zeng, Y. Guo, L. Li, and W. Chen. 2018. Behavior and Three-dimensional Finite Element Modeling of Circular Concrete Columns Partially Wrapped with FRP Strips. *Polymers (Basel)*. 10(3). Doi: 10.3390/polym10030253.
- [23] J. J. Zeng, Y. C. Guo, W. Y. Gao, W. P. Chen, and L. J. Li. 2018. Stress-strain Behavior of Concrete in Circular Concrete Columns Partially Wrapped with FRP Strips. *Compos Struct*. 200: 810-828. Doi: 10.1016/j.compstruct.2018.05.001.
- [24] A. Daou, G. Chehab, G. Saad, and B. Hamad. 2020. Experimental and Numerical Investigations of Reinforced Concrete Columns Confined Internally with Biaxial Geogrids. *Constr Build Mater*. 263. Doi: 10.1016/j.conbuildmat.2020.120115.